Available online at www.sciencedirect.com
SCIENCE DIRECT®
Journal of Electroanalytical Chemistry 579 (2005) 143–152
Journal of Electroanalytical Chemistry
www.elsevier.com/locate/jelechem

Nitrate reduction catalyzed by nanocomposite layer of Ag and Pb on Au(1 1 1)

Seongpil Hwang, Joohan Lee, Juhyoun Kwak *

Department of Chemistry, Korea Advanced Institute of Science and Technology (KAIST), Daejon 305-701, Republic of Korea

Received 10 November 2004; received in revised form 28 January 2005; accepted 3 February 2005
Available online 18 March 2005

Abstract

The underpotential deposition (UPD) of silver and lead on Au(1 1 1) was performed sequentially to produce a thin composite layer. Ag was deposited underpotentially in 1 mM Ag_2SO_4 and 0.1 M H_2SO_4 at 0.400 V and 0.010 V vs. Ag wire. The results of cyclic voltammetry carried out on this Ag/Au(1 1 1) electrode in a Pb^{2+} electrolyte with 0.1 M $HClO_4$ indicated contributions from both Au and Ag substrates. In situ STM images showed that the UPD of Pb on Ag/Au(1 1 1) had an unusual multilayer morphology. Cyclic Voltammetry was also used to demonstrate the stability and presence of the Ag adlayer in the Pb^{2+} electrolyte. In the presence of sodium nitrate, this composite system exhibits a catalytic effect on nitrate reduction that is not observed for Au(1 1 1), Ag/Au(1 1 1), Pb/Au(1 1 1), Ag(1 1 1), or Pb/Ag(1 1 1). Our results demonstrate that the Ag–Pb/Au(1 1 1) composite system has an enhanced catalytic effect on nitrate reduction.

Keywords: Underpotential deposition; Scanning tunneling microscopy; Nanocomposite; Nitrate reduction; Electrocatalyst; Adlayer

1. Introduction

The physicochemical properties of nanocomposite metallic surfaces differ from those of bulk materials due to quantum size effects. Many researchers have studied how the local structure and composition of nanomaterials affect their performance as catalysts. Goodman and co-workers [1] reported that the unusual catalytic activity of gold clusters depends on the thickness of the clusters, and that unique catalytic properties can be achieved when one dimension of the metal becomes smaller than several monolayers.

Composition, as well as size and thickness, can affect the performance of catalysts. In multicomponent electrocatalysts, the properties of the components may contribute to catalysis proportionally to their content if a phase mixture is obtained (known as a bifunctional catalyst), or they may be amplified if an intimate homogeneous mixing between the components is achieved [2]. The manipulation of thickness and composition effects has extraordinary potential for the development of new electrocatalysts.

Thin composite films are commonly used to study the effects of thickness and composition. They also have technological importance as catalysts [3]. Most composite surfaces are manufactured with UHV techniques under high temperatures and low pressures. In contrast, the underpotential deposition (UPD) of metals can produce highly ordered surface structures from the liquid phase under ambient conditions with economical procedures. In addition, the structure, coverage and other phenomena of UPD are well understood [4–6], so precise and deliberate control of surface coverage and structure is possible. However, most UPD studies deal with the deposition of a single metal-ion component

* Corresponding author. Tel.: +82 42 869 2833; fax: +82 42 869 2810.
E-mail address: Juhyoun_Kwak@kaist.ac.kr (J. Kwak).

0022-0728/$ - see front matter © 2005 Elsevier B.V. All rights reserved.
doi:10.1016/j.jelechem.2005.02.004

on a substrate. The co-underpotential deposition of two or more metal ions has received very little attention [7–12], though co-deposition of more than two different metal ions opens up the possibility of fabricating catalytic electrodes. Schmidt and Gygax studied UPD in binary systems and concluded that the partial coverage of the surface with the metal having the more positive peak potential leads to a blocking of surface sites with respect to the deposition of the metal with the more negative peak potential [7]. Stucki [8] studied various co-UPDs of Cu^{2+}, Pb^{2+}, and Ag^{+} on Au. Pauling and Jüttner [9] deposited Ag and Pb on Au(1 1 1) using the dipping technique. In this technique, Ag was deposited under semi-infinite linear diffusion controlled conditions concurrently with the UPD of Pb from the same solution. El-Maksoud et al. [10] reported the co-UPD of copper and zinc on Pt. Smith and Abruña reported the co-adsorption of UPD copper and irreversibly adsorbed bismuth on Pt(1 1 1) and Pt(100) [11]. After bismuth was deposited irreversibly, the electrolyte was replaced with copper solution. Takami et al. [12] demonstrated the formation of a composite monolayer of Ag and Cu on Au(1 1 1) by sequential underpotential deposition. Ag (the more noble metal) was underpotentially deposited, and the modified electrode was then removed from the silver electrolyte and placed in a copper solution. Then, Cu (the less noble metal) was deposited underpotentially. They suggested that the less noble metal does not underpotentially deposit onto the more noble adlayer to prepare a laterally mixed single monolayer. Although, Shima et al. [13] have examined the giant magnetoresistance of ultrathin laminated films fabricated with an electrochemical method, and Fonticelli et al. [14] have reported the variation of surface conductance of composite surfaces, the enhanced catalytic activity of thin composite surfaces fabricated by the co-deposition of two different metals has not yet been reported to the best of our knowledge.

Herein, we demonstrate how the thickness and composition of thin Ag–Pb composites fabricated by using the co-UPD of Ag and Pb on Au(1 1 1) affect nitrate electroreduction. The Pb UPD process on Ag-modified Au(1 1 1) was characterized using cyclic voltammetry with and without the presence of nitrate. We obtained in situ STM images that demonstrated the formation of unusual multilayer morphology during the Pb UPD process. The composite surface was found to catalyze nitrate reduction, which is an important process in the areas of detection and waste remediation, and in the production of useful nitrato compounds [15–19]. Electrocatalytic effects were not observed for any of the Au(1 1 1), Ag(1 1 1), Ag/Au(1 1 1), Pb/Au(1 1 1), or Pb/Ag(1 1 1) interfaces. This is the first example of efficient catalysis by a nanocomposite surface and provides a new method for finding catalysts.

2. Experimental

2.1. Instruments

Voltammetric data were collected using a Pt wire counter electrode and a saturated Hg/Hg_2SO_4 reference electrode (MSE) connected to the electrochemical cell via a capillary salt bridge to minimize contamination from the reference electrode. An Ag wire was used as the reference electrode in the silver UPD experiments. The potential of Ag/Ag^{+} (1 mM) vs. MSE is -0.024 V at room temperature. The solution was purged with Ar prior to use, and an atmosphere of Ar was maintained in the cell during all electrochemical measurements. Potential control and sweeps were established using an Autolab potentiostat (Eco Chemie, Netherlands).

The STM images were obtained in constant current mode with a Topometrix TMX 2000, which was calibrated against a highly ordered pyrolytic graphite (HOPG) surface in air for in-plane dimensions, and against monoatomic Au(1 1 1) steps for dimensions normal to the surface. An electrochemically etched Pt/Ir wire (Molecular Imaging, AR) coated with Apiezon wax or polyethylene was used as the STM tip. A Pb wire served as the reference electrode and a Pt wire was used as the counter electrode. All images in this paper are presented unfiltered.

The nitrite ions, produced by nitrate reduction, were detected with the Griess reaction. The Griess reaction is based on a chemical reaction between sulfanilamide (Aldrich) and *N*-1-napthylethylenediamene dihydrochloride (Aldrich) under acidic conditions. After 30 cycles of potential sweep, 1 mL of electrolyte is mixed with the Griess reagents. The concentration of nitrite ions can then be estimated from the intensity of the purple azo compound, which we determined from the UV absorbance at 520 nm with a Genesys-2 UV–Vis spectrophotometer (Spectyronic).

2.2. Preparation of the Ag–Pb/Au(1 1 1) nanocomposite and Ag(1 1 1)

Ag was underpotentially deposited on a Au(1 1 1) working electrode (Metallhandel Shröer GmbH, Germany) with an electroactive area of 0.283 cm^2, that was annealed with an H_2 flame, in a silver deposition solution consisting of ultrapure water (Modulab, US Filter, >18 MΩ cm), 1 mM Ag_2SO_4 (Aldrich, 99%) and 0.1 M H_2SO_4 (Aldrich, 99.999%). Silver was deposited at 0.400 V vs. Ag wire and at 0.005 V vs. Ag wire. The modified electrode was then removed from the silver electrolyte in air under open circuit control. After rinsing with ultrapure water and drying in a flow of N_2, the electrochemical cell was filled with the second electrolyte solution. Solutions for the Pb adsorption studies

in the absence of nitrate were prepared from ultrapure water and 5 mM PbO (Aldrich, 99.999%). For the Pb adsorption studies in the presence of nitrate, $NaNO_3$ (Aldrich, 99.99%) was added. The supporting electrolyte was 0.1 M $HClO_4$ (Aldrich, Double-distilled). Ag wire was only used in the first step for depositing the silver layer as the reference electrode. Mercury/mercury sulfate (MSE) was used as the reference electrode in the other experiments.

The Ag(1 1 1) electrode was fabricated using the defect mediated growth method [20,21]. Ag was deposited on Au(1 1 1) by potential steps from 50 to 350 mV vs. Pb wire with a frequency of 2 Hz in silver electrolyte prepared from 0.4 mM $AgClO_4$ (Aldrich, 99.9%), 0.1 M $Pb(ClO_4)_2$ (Aldrich, 99.995%) and 0.1 M $HClO_4$. After 2000 cycles (approximately 100 ML of Ag was deposited), the electrode was rinsed with ultrapure water and dried in N_2 gas. The structure of the deposited Ag electrode was shown to be Ag(1 1 1).

3. Results and discussion

3.1. Formation of the nanocomposite by sequential underpotential deposition

Scheme 1 illustrates the sequential procedure for producing the Ag–Pb/Au(1 1 1) nanocomposites. In the first step, the potential of an Au(1 1 1) substrate in a silver deposition solution was cyclically swept from 0.650 V to −0.005 V vs. the Ag wire reference electrode. During the anodic scan, the potential sweep was stopped at 0.400 V to deposit a submonolayer of Ag on Au(1 1 1). The cyclic voltammogram (CV) shown in Fig. 1(a), the in situ STM image at this potential (Fig. 1(b)), and the net charge of deposition (91 μC/cm^2) are in accordance with previously reported results [22,23]. The Ag modified substrate was then transferred to the Pb^{2+} solution for the second UPD step.

Pb UPD was performed in the absence of sodium nitrate on the Ag-modified Au(1 1 1) electrode. The CV of Pb UPD on the Ag-modified Au(1 1 1) (Fig. 2(a)) is different from that on Au(1 1 1) or Ag(1 1 1) [24]. This CV of Pb UPD is similar to that reported for Ag and Pb co-deposition on Au(1 1 1) by Pauling and Jüttner [9], indicating that the Pb UPD is affected by both Au and Ag. They concluded that the cathodic peak at

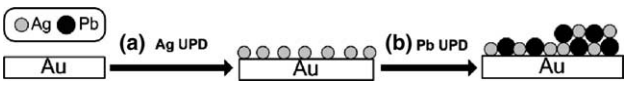

Scheme 1. Illustration of the use of sequential underpotential deposition to produce a Ag–Pb/Au(1 1 1) nanocomposite. (a) First, a submonolayer of Ag is deposited in 1 mM Ag_2SO_4 and 0.1 M H_2SO_4. (b) After the Ag solution is replaced with Pb solution, Pb is deposited on the Ag-modified Au(1 1 1) in 1 mM PbO and 0.1 M $HClO_4$.

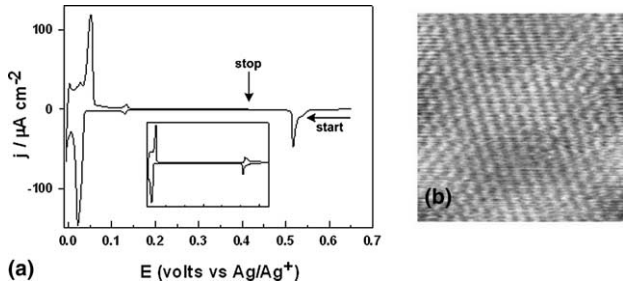

Fig. 1. (a) CV for silver deposition in 0.1 M H_2SO_4 and 1 mM Ag_2SO_4 on Au(1 1 1). The potential was stopped at 0.400 V during the anodic scan. Scan rate = 0.010 V/s. Inset: CV in 0.1 M H_2SO_4 and 1 mM Ag_2SO_4 on Au(1 1 1). (b) In situ STM image of Ag UPD at 0.400 V vs. Ag wire.

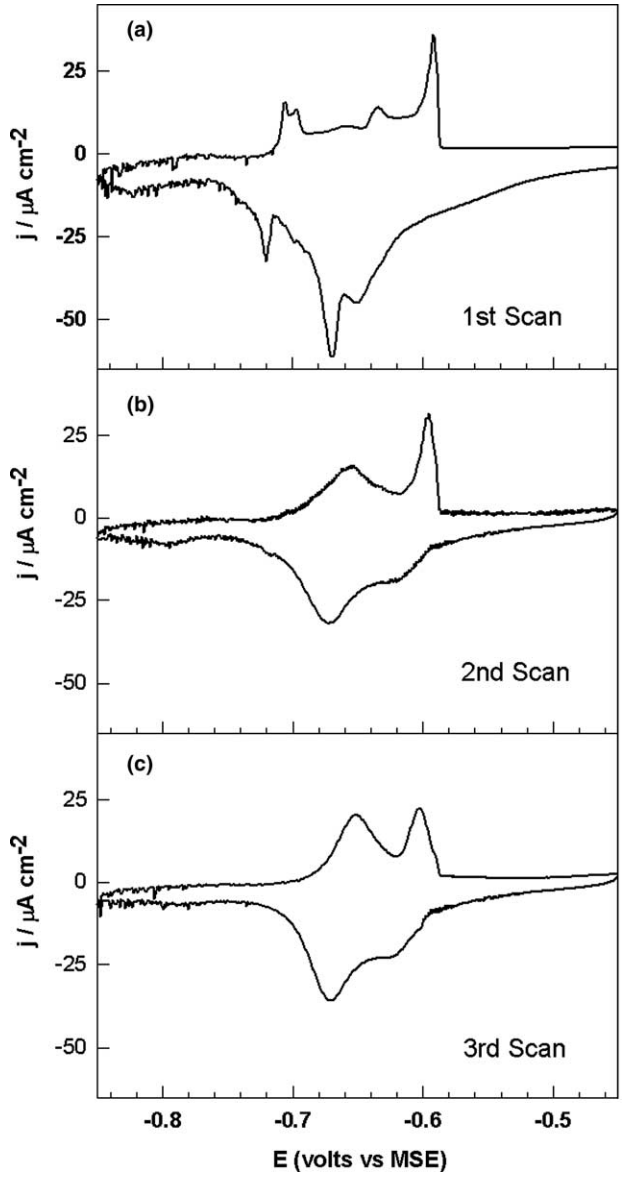

Fig. 2. CVs in 5 mM PbO and 0.1 M $HClO_4$ on partially covered Au(1 1 1). The potential was scanned in the stable Ag region: (a) first scan; (b) second scan; (c) third scan. Scan rate = 0.010 V/s.

−0.720 V corresponding to the anodic peaks at −0.700 V can be attributed to the UPD of Pb on Ag(1 1 1), and that the cathodic peaks at −0.675 V corresponding to the anodic peaks at −0.640 V and, −0.600 V are caused by Pb UPD on Au(1 1 1). During the second and third scans (Fig. 2(b) and (c)), the UPD peaks of Ag around −700 mV disappear, and both the anodic and the cathodic peaks of Au shift to more negative potential. CVs of following potential scan are the same as that of the third scan. The variation in the voltammogram indicates the structural changes in the deposited silver due to deposition and stripping of Pb.

Fig. 3 presents CVs obtained for scans between −850 and 610 mV vs. MSE beginning cathodically at −450 mV. At ~400 mV, the CV exhibits a stripping peak and a weaker deposition peak, corresponding to the removal of Ag atoms and their partial redeposition respectively. After repeated cycling, the Ag atoms were stripped completely, the third CV produced a voltammogram corresponding to Pb UPD on Au(1 1 1) (Fig. 3(c)). The charge of the Ag stripping peak was 71 μC/cm^2. The difference between this stripping charge and that of the deposition in the first deposition step may be due to the change in stability produced by the exchange of electrolyte. The replacement of electrolyte under open circuit conditions may cause the stripping of silver. These results for the silver stripping show that the bulk of the Ag layer on Au(1 1 1) is stable during the Pb UPD process and that the Ag adlayer on Au(1 1 1) results in a Pb UPD voltammogram that is different from that on pure Au(1 1 1).

In order to visualize the Pb UPD process, in situ STM was utilized. The STM image of the Pb-free surface taken at −0.450 V vs. MSE (Fig. 4(a)) shows a number of one atomic height Ag bumps (0.2-nm step), which were not observed on clean Au(1 1 1) at this potential. Sweeping the potential to −0.600 V produced the image shown in Fig. 4(b). The surface was found to be covered with lots of small protrusions, in contrast to the 5–12 nm wide islands on Au(1 1 1) reported at this potential [25–27]. During the acquisition of Fig. 4(c), the electrode potential was changed to −0.650 V. At this potential, the formation of a full Pb monolayer and of several islands in a second layer were observed (Fig. 4(d)). On these islands, the formation of a third layer occurs at −0.700 V as well as the growth at −0.750 V, which are not reported on clean Au(1 1 1); images of these formations are shown in Figs. 4(e) and (f). The image at −0.800 V is identical to that at −0.750 V. Since the catalytic current begins at ~−0.600 V and ends at ~−0.700 V as discussed below, catalytic activity seems to be associated with the second and third layers. In contrast, Pb UPD on clean Au(1 1 1) does not produce such multilayer islands, according to previous reports. [25–27] Thus the morphology of Pb UPD is altered by the presence of a small amount of silver on the surface. This unusual multilayer UPD on the second layer islands after the cathodic peaks at −0.675 V (Fig. 2(a)) indicates that silver atoms are present in the second layer, because lead is underpotentially deposited on Ag in this potential region and on Au before this potential [9].

The lead desorption process was also characterized with in situ STM. After acquisition of Fig. 4, the electrode potential was changed to −0.650 V. At this potential, the desorption of the layer on top of the second layer was observed (Fig. 5(a), arrowed island). This observation also implies the presence of silver atoms on the second layer because lead is desorbed from Ag at this potential. At −0.600 V, lead desorbs from the

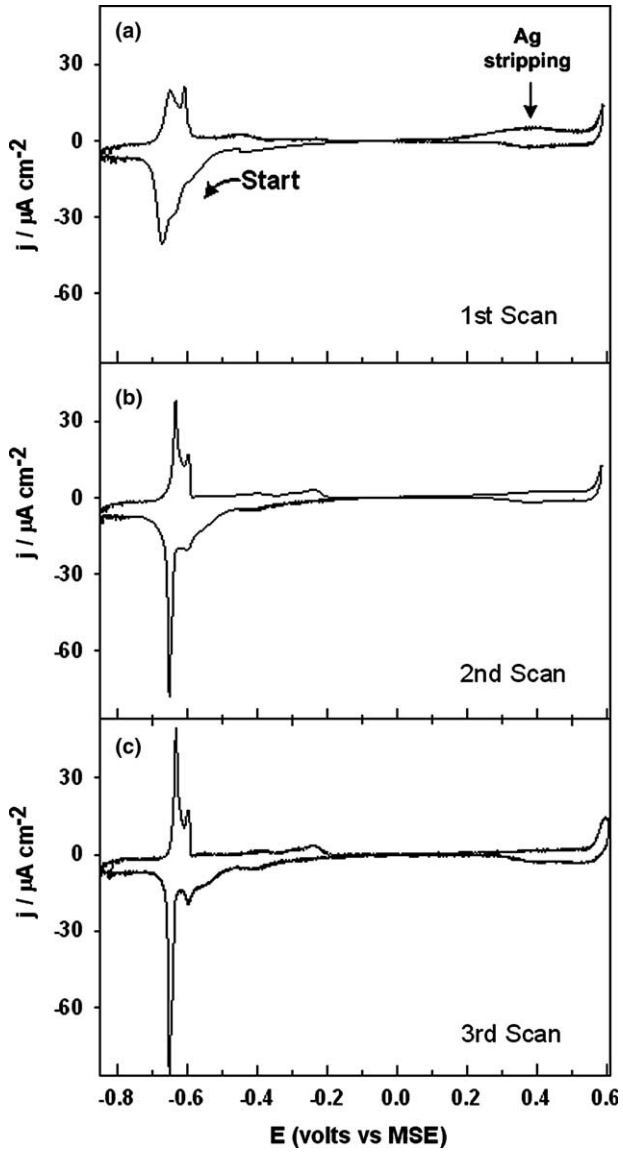

Fig. 3. CVs in 5 mM PbO and 0.1 M $HClO_4$ on partially covered Au(1 1 1). After Fig. 2 was acquired, the potential was scanned beginning cathodically at −450 mV and between −850 and 610 mV vs. MSE to strip the Ag layer: (a) first scan; (b) second scan; (c) third scan. Scan rate = 0.010 V/s.

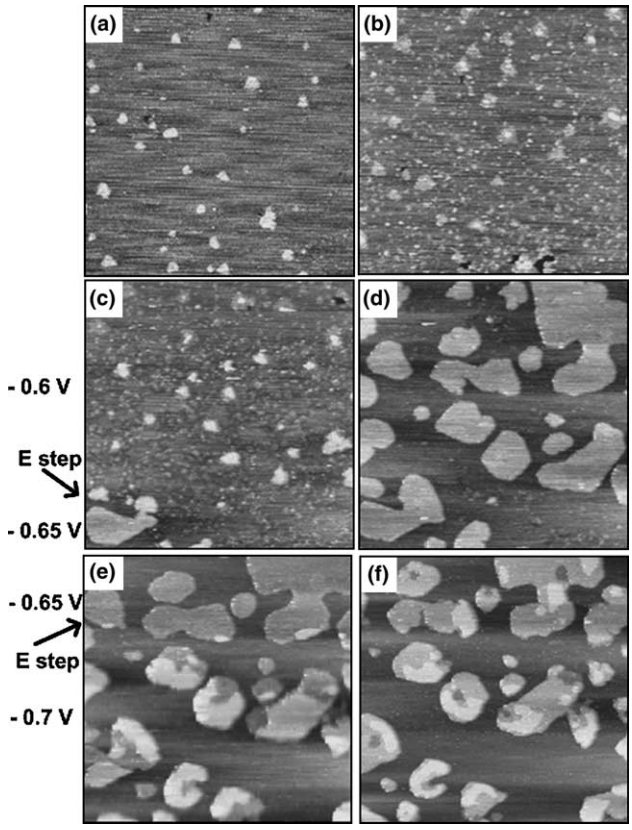

Fig. 4. In situ STM images obtained during Pb UPD on partially covered Au(1 1 1). (a) Image of one atomic height Ag clusters at −0.450 V. (b) Image of small protrusions and Ag clusters at −0.600 V. The electrode potential was changed from −0.600 V to −0.650 V during recording (c) and (d) was acquired at −0.650 V. Deposition of multilayer at −0.700 V (e) and growth at −0.750 V (f). Scan size = 170 nm × 170 nm.

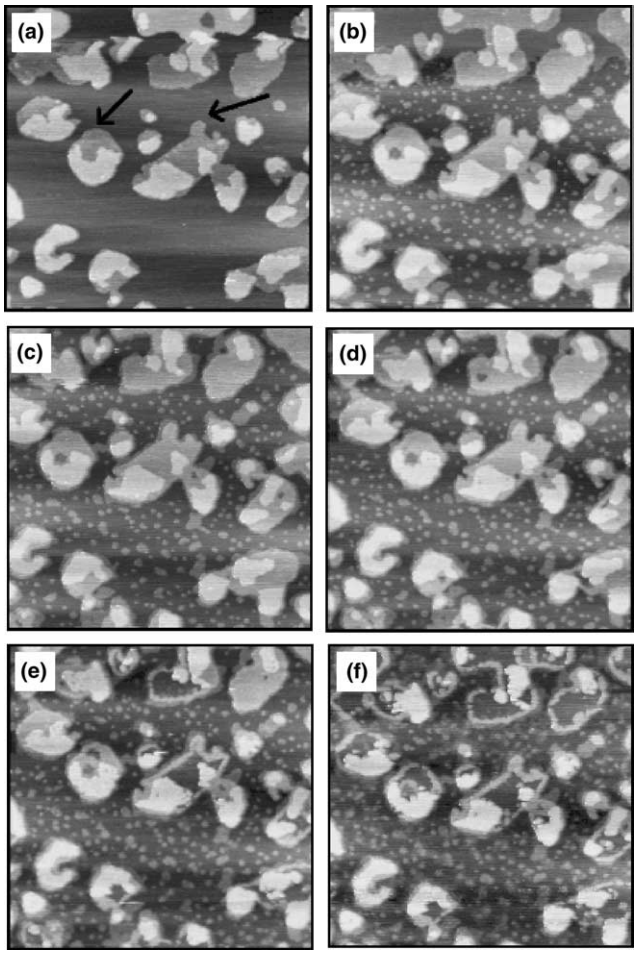

Fig. 5. In situ STM images of desorption of deposited Pb after acquisition of Fig. 4. (a) Image of Pb desorption from the second layer structure at −0.650 V. (b) Image of Pb stripping from the bottom layer, leaving islands at −0.600 V. Images (c) at −0.550 V and (d) at −0.450 V. Desorption from center of the second layer producing ring-like structure (e) at −0.350 V and (f) at −0.250 V. Scan size = 170 nm × 170 nm.

bottom layer, leaving small islands. The multilayer structure of the second layer was maintained. Images at −0.550 V (Fig. 5(c)) and at −0.450 V (Fig. 5(d)) were found to be almost the same as that at −0.600 V. When a more positive potential was applied, the adlayer was stripped out at the center of the second layer, leaving the ring-like structure as shown in Figs. 5(e) and (f). The remaining islands in the bottom layer may be lead, which is not fully stripped. Gewirth and co-workers [27] have reported that lead islands persist until the oxidation of the gold surface. By comparing Fig. 4(a) and Fig. 5(f), the ring-like structures and persisting islands can be seen to have very different morphologies. The significant hysteresis in the deposition and stripping of lead is similar to that found in previous results for Pb UPD on Au(1 1 1) [27]. These variations in surface morphology may cause the changes in the CVs as shown in Fig. 2.

As we noted in the introduction, Takami et al. suggested that the less noble metal must not underpotentially deposit onto the more noble adlayer for fabricating a laterally-mixed single monolayer. They showed that the two kinds of metal form a single monolayer and the less noble metal fills the open spaces in the monolayer created by the more noble metal. In the case we are discussing, however, Pb is underpotentially deposited on both Au and Ag and multilayer deposition was observed by in situ STM. The difference between this case and that discussed in the work of Takami et al. makes the prediction of the present structure more difficult. Depending on the strengths of the specific interactions between the Au substrate and the adsorbate (Ag, Pb) and of the lateral interactions between the deposited metals (Ag, Pb), different types of composite layers may possibly be realized with UPD [9]: (i) a monolayer formation with statistically distributed Ag and Pb (the structure of Ag–Cu/Au(1 1 1) reported in Ref. [9]); (ii) a monolayer formation with well-separated 2D domains; (iii) a sandwich layer structure with Pb on top of Ag or a partial sandwich layer structure with some

Pb on Au; (iv) a 3D alloy that is either an ideal mixture or of defined stoichiometric composition. According to some reports, Pb and Ag do not form alloys under UHV [29] and electrochemical conditions [29], in order to minimize the surface free energy. Pb is generally found on Ag even when Ag is deposited on Pb-covered Au; in particular, the underlying Ag exhibits rapid surface diffusion [20]. This previous result suggests that the second layer (Fig. 4(d)) may be a Pb layer on Ag islands produced by aggregation of Ag bumps (Fig. 4(a)) due to fast surface diffusion. The sandwich layer from these elucidations, however, cannot explain the multilayer formation of composite system, because Pb must deposit underpotentially on Pb adlayer for the multilayer formation. In contrast to reports that Ag and Pb do not alloy, controversial results for Pb UPD experiments on Ag(1 1 1) have suggested that Ag and Pb can alloy. When Pb UPD onto Ag(1 1 1) single crystals was carried out with a voltammetric routine which included extended long-time polarization between the first and third peak of Pb, the structure of the overlayer in relation to the Ag surface is known to change [30,31]. It was suggested that these changes may be because the extended polarization induces the slow transformation of the overlayer into a more stable coverage, which is accompanied by partial desorption into solution [31,32]. These transformations may include a partial exchange between the sites of the substrate and the deposit, leading to incorporation of the Pb atoms into the Ag substrate [31,32], though such site exchange was not reported under UHV conditions [28]. Because the submonolayer of Ag on Au(1 1 1) may be more fragile than in a single crystal, this transformation would not need extended polarization. Then, a 3 D-alloy structure formed by site exchange or a monolayer with mixed metal atoms formed by partial desorption are expected. In that case, the third layer would be Pb UPD on exposed Ag atoms, resulting from site exchange. In our composite system, larger Ag islands would be created by fast surface diffusion under the Pb layer and then site exchange would occur, forming a partial multilayer alloy. The morphology and unusual multilayer deposition of UPD on Ag-modified Au(1 1 1) are obviously different to that produced by UPD on clean Au(1 1 1), although the precise atomic structure and distribution of the two metals of this composite need further study.

3.2. Electrocatalytic nitrate reduction on Ag–Pb/Au(1 1 1) and the origin of the catalytic effects

The catalytic effects of Ag–Pb/Au(1 1 1) on nitrate reduction were investigated in the presence of nitrate. Fig. 6 shows CVs for Pb UPD in the presence of 5 mM sodium nitrate on the Ag-modified Au(1 1 1) electrode. At the onset of the Pb UPD deposition wave (near −0.600 V in Fig. 2 without nitrate), the catalytic

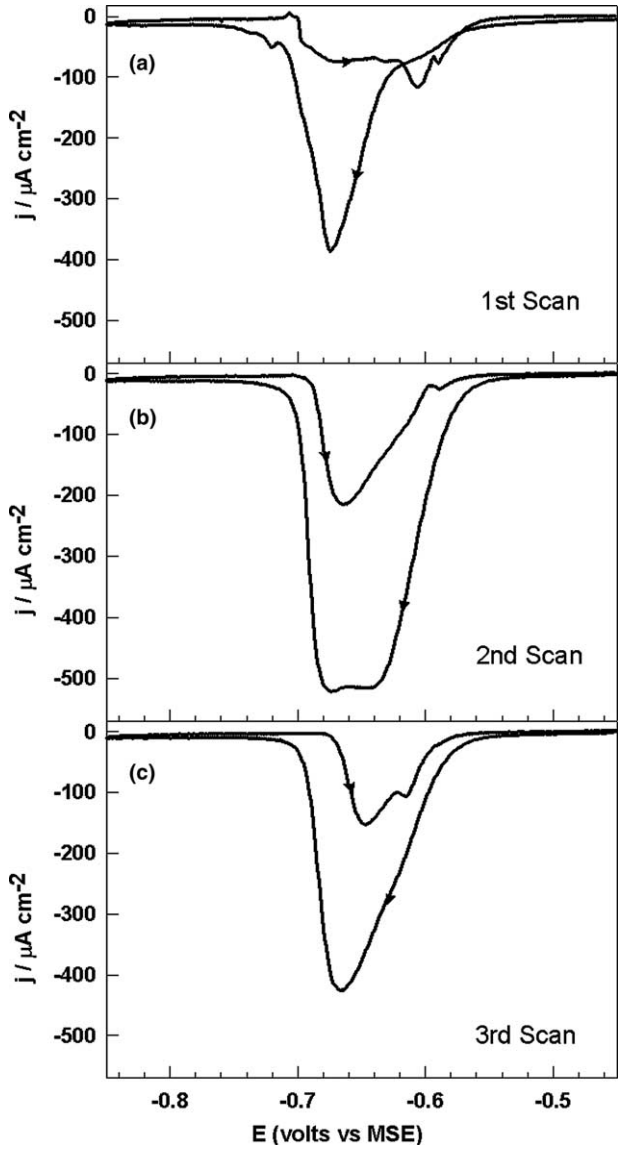

Fig. 6. CVs in 5 mM PbO, 5 mM $NaNO_3$ and 0.1 M $HClO_4$ on partially covered Au(1 1 1): (a) first scan: (b) second scan; (c) third scan. Scan rate = 0.010 V/s.

current rises abruptly. The current suddenly drops to a small value at ∼−700 mV. Catalytic cathodic current is observed during the anodic scan near the potential at which Pb is stripped out, shown in Fig. 2. Similar results were also reported for oxygen reduction catalyzed by Pb/Au(1 1 1) [25]. The shift in peak potential and the change of shape of the CV during repeated scans (Fig. 6(b) and (c)) were also observed in the case without nitrate.

Fig. 7 shows the second sweep of the linear sweep voltammetry, from −0.450 V to −0.850 V, for Pb UPD with 5, 10, and 15 mM sodium nitrate on partially Ag-covered Au(1 1 1). In these experiments, a constant concentration of Pb ions was used while the nitrate concentration of nitrate was varied. The current due to

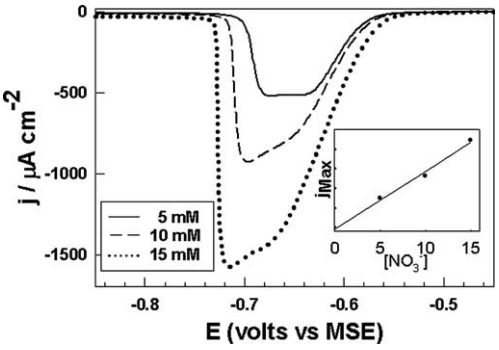

Fig. 7. Linear sweep voltammograms of partially covered Au(1 1 1) swept from −450 mV to −850 mV with various concentrations of nitrate in 5 mM PbO and 0.1 M $HClO_4$: 5 mM $NaNO_3$ (solid line), 10 mM $NaNO_3$ (dashed line), and 15 mM $NaNO_3$ (dotted line). Scan rate = 0.010 V/s. Inset: plot of maximum current as a function of nitrate concentration.

nitrate catalytic reduction was found to increase linearly with the nitrate concentration (see the inset of Fig. 7). This result also demonstrates that the current is catalytic current due to nitrate reduction on the composite electrode.

To confirm the origin of the catalytic effect, the Pb/Au(1 1 1), Ag/Au(1 1 1), and Pb/Ag(1 1 1) systems were tested for their effects on nitrate reduction. Fig. 8(a) shows the CVs for Pb UPD scanned between −0.850 and 0.610 V vs. MSE, beginning cathodically at −0.450 V, in the presence of 5 mM $NaNO_3$ on a Ag-modified Au(1 1 1) electrode. At the onset of the Pb UPD wave, catalytic current was observed. The electrode potential was increased to 0.610 V to dissolve the Ag component. At ~0.400 V, the stripping peak and partial deposition peak of Ag demonstrate the presence of Ag on Au(1 1 1). After removing Ag from the Au substrate, the CV corresponding to Pb UPD on Au(1 1 1) (Fig. 8(c)) reappears. The catalytic effect of Pb UPD on nitrate reduction disappears in 5 mM nitrate solution, though weak catalytic reduction of nitrate has been reported at higher nitrate concentrations [33]. This result shows that Ag is an essential element in electrocatalytic nitrate reduction, i.e. a trimetallic composition (Ag, Pb, Au) is crucial for nitrate electroreduction.

An Ag-modified Au(1 1 1) electrode in the absence of Pb^{2+} exhibits a relatively small cathodic current and negative potential shift in the hydrogen evolution region, as shown in Fig. 9, indicating the role of Pb in the catalytic effect. Since the Pb/Ag interface is one of the possible origins of the catalytic effect, Pb UPD on Ag(1 1 1) was performed. An Ag (1 1 1) electrode was made using defect mediated growth [20,21]. The CV of this electrode in 5 mM PbO + 0.1 M $HClO_4$ is nearly identical with that previously reported for Ag(1 1 1) [24]. When 5 mM sodium nitrate was added, a relatively weak catalytic current was observed, as shown in Fig.

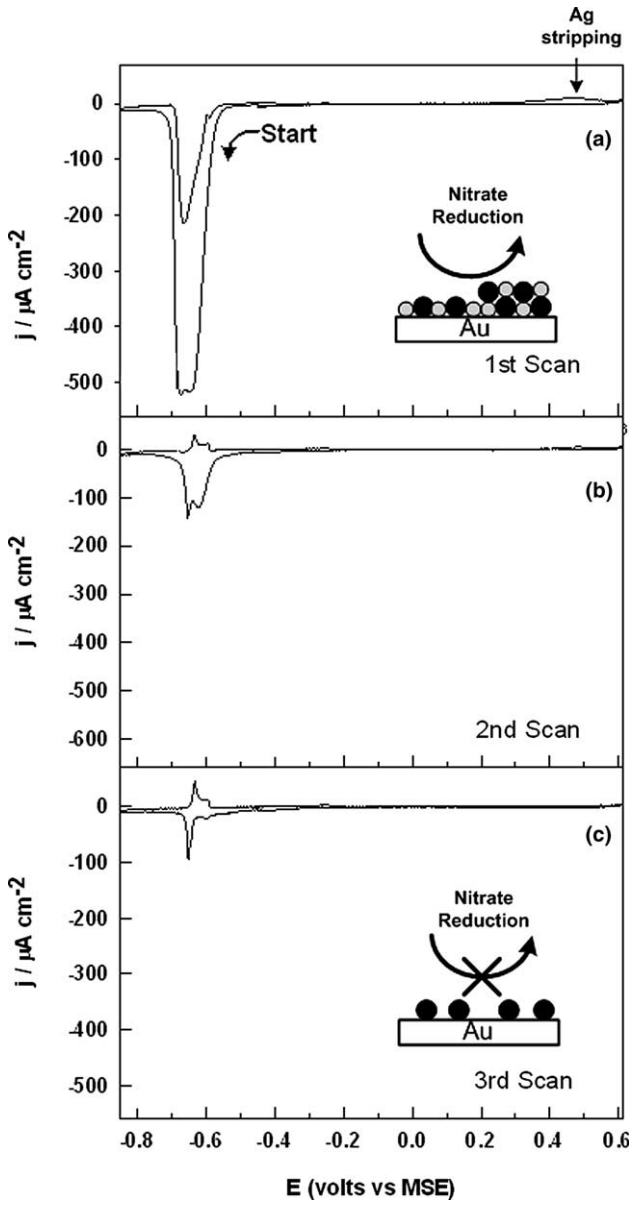

Fig. 8. CVs of stripping of Ag in 5 mM PbO, 5 mM $NaNO_3$ and 0.1 M $HClO_4$: (a) first scan; (b) second scan; (c) third scan. These CVs were acquired beginning cathodically at −450 mV for the same conditions as used in Fig. 6. Scan rate = 0.010 V/s.

10, which is in good agreement with previous reports [34]. This weak current for Pb/Ag(1 1 1) shows that the Ag atomic layer on Au is an important component of the catalytic effect of the composite layer. The results for Pb/Au(1 1 1) (Fig. 8), Ag/Au(1 1 1) (Fig. 9), and Pb/Ag(1 1 1) (Fig. 10) verify that the thin and trimetallic composition of Ag–Pb/Au(1 1 1) is required to catalyze nitrate electroreduction.

Colorimetric detection of nitrite, which is one of the possible products of nitrate reduction, with well-known Griess reaction [35] was also used to verify the unique catalytic properties of the composite. After electrolysis

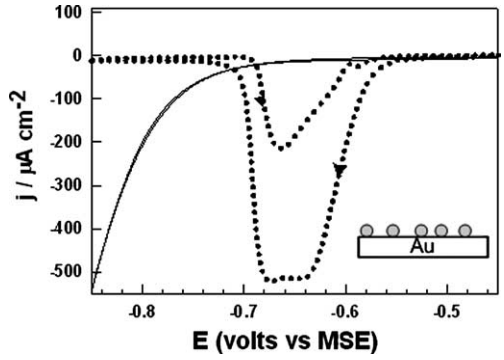

Fig. 9. CVs for partially covered Au(1 1 1) with and without Pb^{2+}: in 5 mM $NaNO_3$ and 0.1 M $HClO_4$ (solid line); and in 5 mM PbO, 5 mM $NaNO_3$ and 0.1 M $HClO_4$ (dotted line). Scan rate = 0.01 V/s.

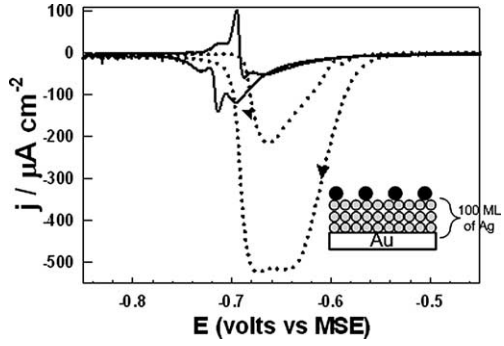

Fig. 10. CV for Pb UPD on Ag (approx. 100 ML, scheme in inset), which was deposited on Au(1 1 1) by defect mediated growth, in 5 mM PbO, 0.1 M $HClO_4$ and in 5 mM $NaNO_3$ (solid line); the dotted lined CV is the same as that in Fig. 10. Scan rate = 0.01 V/s.

was performed with 30 cycles of potential sweep from −0.450 V to −0.850 V vs. MSE on various electrodes at 0.050 V/s, color changes of the electrolytes occur due to the Griess reaction, as displayed in Fig. 11. The electrolyte for Ag–Pb/Au(1 1 1) produce the most intensive colorimetric change while the colors of other electrolytes were unchanged at all except that of the electrolyte for Ag. The color change to purple shows that Ag–Pb/Au(1 1 1) system is the best catalyst to produce nitrite and Ag electrode is a weak catalyst in this potential region [36]. The concentration of nitrite, as determined from the UV absorbance at 520 nm, shows that Ag/Au(1 1 1) catalyzes the production of nitrite only very weakly, and that during electrolysis on Ag–Pb/Au(1 1 1), 97% of the charge is consumed on the production of nitrite ions via one electron reduction. The results of the CVs and for the color changes verify that the thin and trimetallic composition of Ag–Pb/Au(1 1 1) is required to catalyze nitrate electroreduction.

Chronoamperometry (CA) experiments were performed to investigate the enhancement of nitrate reduction current in the absence of Pb cations in solution; the results are shown in Fig. 12. Ag and Pb were deposited at 0.01 V vs. Ag wire and at −0.675 V vs. MSE sequentially. After cleaning with deionized water, the electrochemical cell was filled with 30 mL solution of 5 mM $NaNO_3$ and 0.1 M $HClO_4$. The electrode potential was stepped from −0.850 V to −0.800 V vs. MSE and 1 mL of 30 mM $NaNO_3$ solution was injected to raise the nitrate concentration by ∼1 mM per injection. The CA results for the bare Au(1 1 1) electrode did not undergo any variation after injection, whereas the Ag–Pb/Au(1 1 1) electrode exhibited enhanced reduction current after injection. These results again demonstrate the catalytic effect of deposited Ag–Pb/Au(1 1 1) in the absence of Pb cations in solution.

3.3. Effects of Ag coverage on nitrate reduction

How do the catalytic effects vary with the coverage of Ag? To answer this question, we varied the stop potential. In the first step, the potential of the Au(1 1 1) substrate was swept from 0.650 V to −0.005 V vs. the Ag wire reference electrode at 0.01 V/s. During the potential

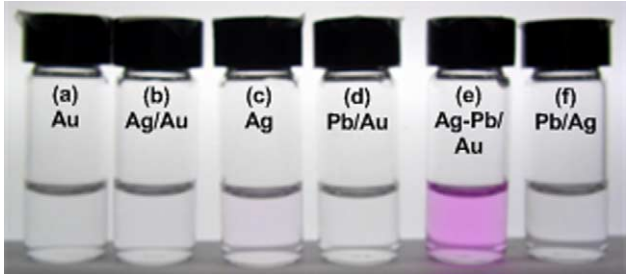

Fig. 11. Photograph showing the color changes of the electrolyte. 30 cycles of electrolysis was performed in 30 mL of solution on: (a) Au, (b) Ag (0.005 V)/Au, (c) Ag (100 ML)/Au (d) Au, (e) Ag (0.005 V)/Au and (f) Ag (100 ML)/Au. The solution consisted of 15 mM $NaNO_3$ and 0.1 M $HClO_4$ for (a)–(c) and 1 mM PbO, 15 mM $NaNO_3$ and 0.1 M $HClO_4$ for (d)–(f). 1 mL of electrolyte was mixed with the Griess reagents. The intensity of the purple indicates the concentration of nitrite ions.

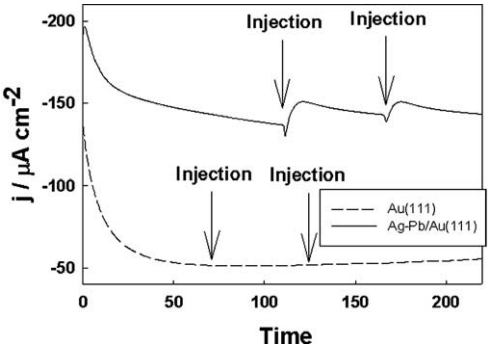

Fig. 12. Current response recorded during the potential step from −0.850 V to −0.800 V vs. MSE for Ag–Pb/Au(1 1 1) (solid line) and bare Au(1 1 1) (dashed line) in 30 mL solution of 5 mM $NaNO_3$ and 0.1 M $HClO_4$. 1 mL of 30 mM $NaNO_3$ was injected to increase the concentration of nitrate.

cycle, the potential was stopped at 0.010 V during the cathodic scan (see the inset of Fig. 13(a)). The net charge of deposition up to 0.010 V was 283 μC/cm^2. After the stop at 0.010 V, the Ag-modified substrate was transferred to the second electrolyte.

Fig. 13 shows the CVs for Pb UPD in the absence of sodium nitrate on a fully covered Au(1 1 1) electrode (2 ML of Ag on Au(1 1 1)), which are similar to that for the partially covered Au electrode (Fig. 2(a)). However, the cathodic peak at −0.720 V and the anodic peaks at −0.700 V, attributed to the UPD of Pb on Ag(1 1 1), are larger than the peaks for the partially covered system. These increase in height of these peaks with the increase in Ag coverage also demonstrates that they

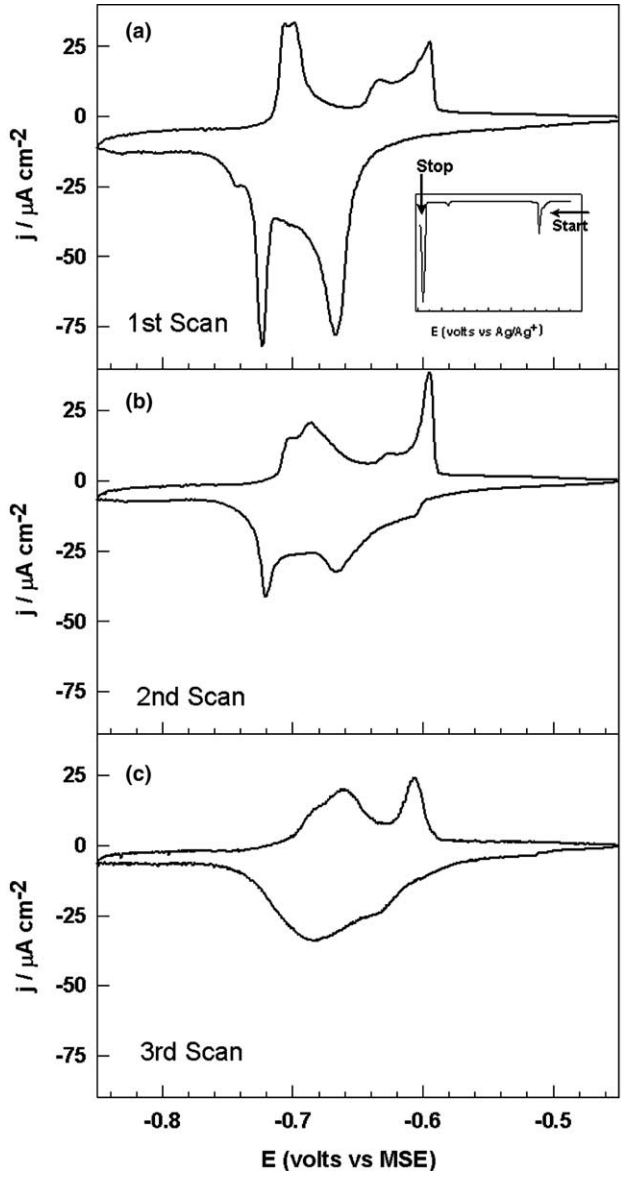

Fig. 13. CVs on Ag-modified Au(1 1 1) (at 0.010 V) for the same conditions as used for Fig. 2 except Ag coverage: (a) first scan; (b) second scan; (c) third scan. Scan rate = 0.010 V/s. Inset: CV for silver UPD deposited at 0.010 V.

are due to Ag, because the increase in Ag adsorbate increases the size of these peaks. The cathodic peaks at −0.675 V and the anodic peaks at −0.640 and −0.600 V, related to Pb UPD on Au(1 1 1), are similar to those of the previous system. The complete coverage of the surface with Ag does not fully block the interactions of Pb with the Au substrate. The in situ STM images obtained during these process are similar to those of partially modified Au(1 1 1). Fig. 14 shows the CVs of the first and second scans for Pb UPD on fully covered Au(1 1 1) in the presence of 5 mM sodium nitrate. The higher current due to nitrate electroreduction is seen in second scan. Changes in the CVs with repeated scans were also observed, as shown in Fig. 6. Compared to the well-known Cd/Au system, this Pb UPD on Au(1 1 1) fully covered with Ag produces more effective catalytic current at low nitrate concentrations (see Table 1).

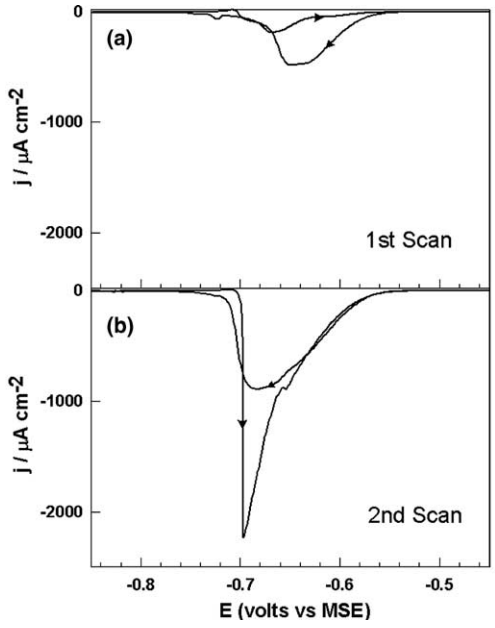

Fig. 14. CVs on Ag-modified Au(1 1 1) (at 0.010 V) in 5 mM PbO, 5 mM $NaNO_3$ and 0.1 M $HClO_4$: (a) first scan; (b) second scan. Scan rate = 0.010 V/s.

Table 1
Maximum current density for nitrate reduction catalysis on different surfaces

Adlayer systems	$[NO_3^-]$ (mM)	J_{max} (μA/cm^2)
Cd/Au[a]	50	637
Pb/Ag[b]	5	124
Ag (at 0.4 V)–Pb/Au[c]	5	530
Ag (at 0.010 V)–Pb/Au[d]	5	883

[a] From Ref. [15].
[b] From Fig. 10.
[c] From Fig. 6(b).
[d] From forward scan in Fig. 14.

Ag is a good promoter of nitrate reduction on Pt and Pd due to its ability to reduce nitrate via a redox reaction [18]. Pb UPD on Au and Ag catalyzes nitrate reduction at high nitrate concentrations [33,34]. The role of each adsorbate in this process has however not yet been determined. Further experiments using active site blocking, EC-STM, and surface IR would be expected to provide more detailed information about the mechanism. If the mechanism were able to provide us with information about composite ratio and structure for catalytic effects, the best catalyst can be achieved by UPD which enable us diverse structure and coverage of metal adlayer.

In the present study, we have demonstrated that a composite layer consisting of two different elements, Ag and Pb, can be produced on Au(1 1 1) with the sequential UPD procedure. Our results show that a composite layer of several monolayers thickness is a useful catalyst for nitrate reduction, which cannot be achieved with monometallic thin films, and that sequential UPD is an easy method for fabricating this kind of composite. The role of Ag in monolayer thick films is entirely different from that in the bulk phase (100 ML). The role of the Ag–Pb composite is also different from that of single element Ag or Pb on Au. The structure of the composite layer is unclear, so a more detailed investigation of the structure is required. However, this strategy can also be applied to fabricate catalysts for other important reactions such as oxygen reduction, carbon dioxide reduction, and methanol oxidation.

4. Conclusion

A composite surface layer consisting of Ag and Pb can be produced on Au(1 1 1) by a solution-phase electrochemical method known as sequential underpotential deposition. From submonolayers to monolayers of Ag and Pb on Au(1 1 1) can be deposited underpotentially in series. The in situ STM images we obtained show the unusual multilayer morphology of these structures. The voltammograms of Pb UPD on Ag-covered Au(1 1 1) are affected by both the Au and the Ag substrates even in the case of full Ag coverage. These composite systems exhibit catalytic effects on nitrate reduction which are not observed for Au(1 1 1), Ag/Au(1 1 1), Pb/Au(1 1 1), Ag(1 1 1), or Pb/Ag(1 1 1). This method provides a route for the synthesis of new bimetallic adlayers on substrates which have possible electrocatalytic properties and atomically tailored interfacial properties.

Acknowledgements

This work was supported by the Korean Ministry of Science and Technology through National R&D Project for Nano Science and Technology and partially by Brain Korea 21 and MICROS.

References

[1] M. Valden, X. Lai, D. Goodman, Science 281 (1998) 1647.
[2] E. Casado-Rivera, D.J. Volpe, L. Alden, C. Lind, C. Downie, T. Vazquez-Alvarez, A.C.D. Angelo, F.J. DiSalvo, H.D. Abruña, J. Am. Chem. Soc. 126 (2004) 4043.
[3] R. Adzic, in: J. Lipkowski, P.N. Ross (Eds.), Electrocatalysis, Wiley-VCH, New York, 1998, p. 197.
[4] A.A. Gewirth, B.K. Niece, Chem. Rev. 97 (1997) 1129.
[5] E. Herrero, L.J. Buller, H.D. Abruña, Chem. Rev. 101 (2001) 1897.
[6] E. Lamy-Pitara, J. Barbier, App. Catal. A 149 (1997) 49.
[7] E. Schmidt, H.R. Gygax, Helv. Chim. Acta 49 (1966) 1105.
[8] D. Stucki, J. Electroanal. Chem. 80 (1977) 375.
[9] H.J. Pauling, K. Jüttner, Electrochim. Acta 37 (1992) 2237.
[10] S.A.A. El-Maksoud, S. Taguchi, T. Fukuda, A. Aramata, Electrochim. Acta 41 (1996) 1947.
[11] S.P.E. Smith, H.D. Abruña, J. Phys. Chem. B 103 (1999) 6764.
[12] S. Takami, G.E. Jennings, P.E. Laibinis, Langmuir 17 (2001) 441.
[13] M. Shima, L. Salamanca-Riba, R.D. McMichael, T.P. Moffat, J. Electrochem. Soc. 149 (2002) C439.
[14] M.H. Fonticelli, D. Posadas, R.I. Tucceri, J. Electroanal. Chem. 565 (2004) 359.
[15] S. Hsieh, A.A. Gewirth, Langmuir 16 (2000) 9501.
[16] F. Epron, F. Gauthard, C. Pineda, J. Barbier, J. Catal. 198 (2001) 309.
[17] S. Kerkeni, E. Lamy-Pitara, J. Barbier, Catal. Today 75 (2002) 35.
[18] F. Gauthard, F. Epron, J. Barbier, J. Catal. 220 (2003) 182.
[19] D. Pittois, G. Kokkinidis, C. Buess-Herman, J. Electroanal. Chem. 532 (2002) 277.
[20] K. Sieradzki, S.R. Brankovic, N. Dimitrov, Science 284 (1999) 138.
[21] S. Hwang, I. Oh, J. Kwak, J. Am. Chem. Soc. 123 (2001) 7176.
[22] V. Rooryck, F. Reniers, C. Buess-Herman, G.A. Attard, X. Yang, J. Electroanal. Chem. 482 (2000) 93.
[23] M.J. Esplandiu, M.A. Schneeweiss, D.M. Kolb, Phys. Chem. Chem. Phys. 1 (1999) 4847.
[24] M.F. Toney, J.G. Gordon, M.G. Samant, G.L. Borges, O.R. Melroy, D. Yee, L.B. Sorensen, J. Phys. Chem. 99 (1995) 4733.
[25] I. Oh, A.A. Gewirth, J. Kwak, J. Caltal. 213 (2003) 17.
[26] M.P. Green, K.J. Hanson, D.A. Scherson, X. Xing, M. Richter, P.N. Ross, R. Carr, I. Lindau, J. Phys. Chem. 93 (1989) 2181.
[27] C.H. Chen, N. Washcurn, A.A. Gewirth, J. Phys. Chem. 97 (1993) 9754.
[28] G. Rosenfeld, R. Servaty, C. Teichert, B. Poelsema, G. Comsa, Phys. Rev. Lett. 71 (1993) 895.
[29] S.R. Brankovic, N. Dimitrov, K. Sieradzki, Electrochem. Solid Struct. 2 (1999) 443.
[30] H. Siegenthaler, K. Jüttner, Electrochim. Acta 24 (1979) 109.
[31] E. Schmidt, H. Siegenthaler, J. Electroanal. Chem. 150 (1983) 59.
[32] N. Dimitrov, A. Popov, T. Vitanov, E. Budevski, Electrochim. Acta 39 (1994) 957.
[33] J. Garcia-Domenech, M.A. Climent, A. Aldaz, J.L. Vazquez, J. Clavilier, J. Electroanal. Chem. 159 (1983) 223.
[34] C. Mayer, K. Jüttner, W.J. Lorenz, J. Appl. Electrochem. 9 (1979) 161.
[35] P. Griess, Ber.Dtsch. Chem. Ges. 12 (1879) 426.
[36] M. Fedurco, P. Kedzierzawski, J. Augustynski, J. Electrochem. Soc. 146 (1999) 2569.